Journal of the Civil Engineering Forum, May 2024, 10(2):199-208
DOI 10.22146/jcef.10316
Available Online at https://jurnal.ugm.ac.id/v3/jcef/issue/archive

Seismic Vulnerability Assessment of Regular and Vertically Irregular Residential Buildings in Nepal

Satish Paudel[1*], Taufiq Ilham Maulana[2], Hakas Prayuda[2]
[1]Department of Civil and Environmental Engineering, University of Nevada, Reno, UNITED STATES
[2]Department of Civil Engineering, Faculty of Engineering, Universitas Muhammadiyah Yogyakarta
Jalan Brawijaya, Tamantirto, D.I. Yogyakarta, INDONESIA
*Corresponding author: satishp@unr.edu, paudelsatish@gmail.com

SUBMITTED 30 October 2023 **REVISED** 08 February 2024 **ACCEPTED** 13 March 2024

ABSTRACT The need to assess the vulnerability of non-engineered residential RCC buildings in Nepal has become urgent, especially considering the ongoing modifications and additions to these structures without understanding their susceptibility to seismic events. Many residential buildings, particularly those up to three stories, did not fully comply to the guidelines outlined in Nepal Building Code NBC 105:2020. Therefore, there is a necessity to assess the seismic performance of these structures. This study aims to quantify the seismic vulnerability of such buildings by focusing on three distinct types: regular two and three-story structures, and irregular three-story structures. Using finite element modeling, the analysis of the buildings' seismic capacity was performed through pushover analysis. Subsequently, linear time history analysis is conducted to determine the seismic demand. Two software were utilized to conduct the analyses, namely SAP2000 and STERA_3D. The study also includes the matching eleven strong ground motion inputs to Nepal's site characteristics and response spectrum to ensure the relevance of the local context. Furthermore, fragility curves are constructed to compare the probability of structural failure, by first conducting the nonlinear dynamic analyses on the building specimens. The result showed that the probability of complete failure rises rapidly when an additional story is constructed with vertical irregularity, increasing from 1.8% to 5.7% in a non-engineered two-story building. The study also observes variations in top displacement across all three buildings due to differences in earthquake duration and frequency. From the findings, it is revealed that a significant increase in seismic vulnerability for vertically irregular buildings compared to regular ones.

KEYWORDS Seismic Vulnerability; Performance Based Design; Fragility Curve; Irregular Structure; Residential Building

1 INTRODUCTION

Situated between the Indian and Eurasian plates, Nepal is highly prone to seismic activity. The convergence of these plates has historically led to devastating earthquakes, including notable ones in 1833, 1934, and 1505, with magnitudes exceeding M8. Particularly, the 1934 Nepal-Bihar earthquake claimed over 10,000 lives in the Kathmandu Valley alone. The more recent Gorkha Earthquake in 2015, measuring M7.8, followed by a M7.3 aftershock, resulted in 8,790 deaths and extensive damage to around 800,000 residential buildings (NPC, 2015). The root cause of this catastrophic destruction is attributed to the proliferation of non-engineered constructions. Since the 1990s, there has been an unchecked surge in building construction in Nepal, often without adherence to safety standards. Recognizing this issue, the government introduced the National Building Code in 1994, emphasizing the concept of 'Pre-Engineered Buildings' to simplify construction for homeowners. These buildings are constructed based on predetermined specifications, encompassing both structural and non-structural elements, such as dimensions and reinforcement details. Compliance with these specifications exempts buildings from requiring design and supervision by professional engineers. Despite the introduction of the National Building Code, lax enforcement by the government has led to the prevalence of non-engineered constructions over pre-engineered ones. The phenomenal rise in remittance resulted in a significant increase in the living standard of Nepalese people after 2000 A.D (World Bank, 2017). Indeed, the abundance of Reinforced Cement Concrete (RCC) houses was found in the country, constructed without adhering to the specified detailing criteria outlined in Nepalese or Indian building codes, making them non-engineered structures. The most common building layout was a two-story house with 2-bay in one direction and 3-bay in another direction. However, with a constant increase in economic status and the rising value of land, people got keen on adding another story above the constructed one making the structure vertically irregular in the name of constructing Two and a half story building in layman's terms. The term 'vertically irregular' is defined according to Indian Standard (I.S.) 1893:2016 (Indian Standard, 2016). This paper attempts to compare the seismic vulnerability of the regular two-story non-engineered building, vertically irregular three-story non-engineered building (i.e. *so-called Two and a half story building in layman's terms*), and regular three-story non-engineered building.

Numerous studies have been conducted after the Gorkha earthquake to determine the seismic vulnerability of the structures using several techniques. Damage probability matrices and empirical fragility functions were determined for traditional vernacular masonry structures likely to collapse in strong ground motions using a database of past earthquakes (Gautam and Rodrigues, 2018). Damage assessment of cultural heritage was done through a case study by performing the linear static analysis (Shrestha et al., 2017). The vulnerability of historical structures was assessed using a refined distinct element method and numerical modeling of the structure, further followed by field verification (Kiyono et al., 2017). The seismic vulnerability was determined using the rapid visual screening method and fragility curve method for traditional masonry buildings (Basukala and Maskey, 2017). The behavior of structural elements when subjected to significant lateral cyclic deformation is intricate, prompting numerous full-scale tests to gain insights into their seismic performance (Paudel et al., 2022*a*,*b*). Extensive laboratory experiments have deepened researchers' understanding of various structural systems, ensuring their safety and reliability under diverse load conditions. Nevertheless, conducting full-scale structural load tests demands considerable time and financial resources. Thus, simulations offer a viable alternative for investigating composite structure behavior and refining design equations for seismic loading scenarios. Numerical simulation stands out as a promising method to design and evaluate structures with intricate configurations under seismic forces (Tanapornraweekit et al., 2022; Paudel, 2023). Additionally, several machine learning techniques have been adopted to assess the relationship among several parameters, which can also be adopted to assess the behavior of the structure (Paudel, 2023).

In 1994, the Nepal National Building Code (NBC 105:1994) was formulated to address seismic design, yet its implementation faced challenges until 2003 (NBC, 1994*a*). Despite its presence, certain areas of the country remained vulnerable due to inadequate standards, as noted by various researchers (Bhusal et al., 2023). Recognizing the shortcomings, the Government of Nepal introduced the Nepal Building Code (NBC 205:1994) (NBC, 1994*b*), later updated to NBC 205:2012 (NBC, 2012), commonly known as the Mandatory Rule of Thumb (MRT), aiming to improve construction practices and minimize the risks associated with hasty reinforced concrete (R.C.) building construction. Technicians and contractors could readily adopt this standard without the design from the structural designers. However, the revision in 2012 focused solely on MRT (NBC 205:2012) without updating the seismic design standard (NBC 105:1994). The devastating Gorkha earthquake in 2015 underscored the urgent need to revise the seismic design code. Consequently, NBC 105:2020 (NBC, 2020) was developed in response to this earthquake, setting new standards for seismic load estimation and earthquake-resistant construction practices. Despite the widespread adoption of NBC 205:2012, many residential buildings, particularly those up to three stories, did not fully adhere to the guidelines outlined in NBC 105:2020. Therefore, there is a necessity to assess the seismic performance of these structures. The salient features and important geometric properties of the buildings that are usually constructed in Nepal are shown in Table 1.

Table 1. Basic features and geometry of building typologies constructed in Nepal

Description	Buildings specifications	Code compliance (NBC 205)
No. of stories	2 and 3	Up to 3 Story
Total height H (m)	6 and 9	< 11 m
Story height h (m)	3.0	-
No. of bays	2×3 and 3×3	< 6
Length, A (m)	10.2	< 25.0 m, A < 3B
Breadth, B (m)	9	< 25.0 m, B < 3A
H/A, H/B	0.6, 0.7 and 0.9, 1.0	< 3
Plinth area (sq. m)	91.8	

The non-engineered RCC buildings that remain standing after the Gorkha Earthquake have raised significant concerns for designers: Are they safe for the next earthquake? What is its seismic vulnerability state? Not only are current non-engineered buildings susceptible on their own, but they also have the potential to heighten the vulnerability of neighboring structures. Moreover, people are increasingly adding another story with vertical irregularity above existing structures. Hence, this paper aims to quantify the existing seismic vulnerability state of these buildings and compares it with the vulnerability when an additional story is added irregularly and regularly. The findings of this paper will be beneficial for middle-class homeowners adding another story to their existing structure.

2 METHODOLOGY

A typical non-engineered RCC building of two stories was selected for analysis. The building fell under the category of R.C. buildings with ordinary moment-resisting 'frame' according to IS 1893: 2016 (Indian Standard, 2016) and NBC 105:2020 (NBC, 2020) standards. As it did not comply with the norms of ductile detailing outlined in IS 13920 (Indian Standard, 1993), it was classified as an ordinary moment-resisting frame. Numerical modeling of the building was performed using the finite element method on structural analysis software, SAP 2000 version 24 and STERA_3D (Saito, 2020). These tools are widely used to investigate the seismic behavior of reinforced concrete and masonry structures (Bhusal and Paudel, 2021; Bhusal et al., 2020; Bhusal and Paudel, 2021; Motra and Paudel,

Table 2. Limit strain for concrete and steel (acceptance limits)

Limits	Concrete strain	Steel strain
I.O.	$(\varepsilon c)\, IO = 0.0035$	$(\varepsilon c)\, IO = 0.0035$
LS	$(\varepsilon c)\, LS = 0.0035 + 0.01 \left(\frac{\rho s}{\rho sm}\right) \leq 0.0135$	$(\varepsilon s)\, LS = 0.04$
CP	$(\varepsilon c)\, LS = 0.004 + 0.013 \left(\frac{\rho s}{\rho sm}\right) \leq 0.018$	$(\varepsilon s)\, CP = 0.06$

2021; Paudel and Bhusal, 2021). The capacity of the building was determined through displacement-controlled pushover analysis. This analysis technique employed a simplified non linear method within a static framework to predict seismic structural deformations. It evaluated the structural behavior by approximating both the force and deformation capacity through a non-linear static analysis algorithm. Additionally, it provided insights into the sequence of yielding members and the advancement of the overall capacity curve. Hinges in models were defined according to the guidelines of ASCE 41-17 (ASCE, 2017).

In the context of non-linear modeling using SAP 2000 version 24 and STERA_3D, various hinge options are available including auto/default hinge, user-defined hinge, and fiber hinge. The auto and user hinge utilize moment- curvature *(M_3)* for beams and P-M_2-M_3 for columns. The analysis of the auto hinge is based on assigned material, section, and reinforcement details. The user-defined hinge allows users to generate moment-curvature and interaction curves for custom hinge behavior. To represent cracked section behavior, beam and column moment of inertia values were estimated as $0.35I_g$ and $0.70I_g$, respectively (ACI, 2014). The plastic hinge length was determined as 0.5 times the cross-section depth based on ATC-40 (ATC, 1996). For macro modeling depicting non-linear behavior, hinge definition is crucial. The default hinge uses yield values and estimates other parameters based on yield properties and code provisions without considering material stress-strain behavior. The fiber hinge discretizes the element into uniaxial fibers with different stress-strain behavior based on defined material, recommended for capturing non-linear behavior. Parametric studies varied hinge length, with 10% of structural member length showing optimal accuracy and computational time, as adopted in this study and suggested in SAP 2000 version 24 and STERA_3D. In STERA_3D, the modeling approaches were similar to SAP 2000, where for the structural elements such as beam and columns, the non linear flexural springs were modeled at both ends of the member, while the non linear shear spring was modeled at the middle of the structural members. The details of STERA_3D modeling methods can be found in the STERA_3D Manual (Saito, 2020). Acceptance limits were determined based on TEC 2007 (TEC, 2007) for performance evaluation, including minimum sectional damage boundary (M.N.), sectional security bound (G.V.), and section collapse bound (G.C.) for immediate occupancy (I.O.), life safety (L.S.), and collapse prevention (C.P.) limits and shown in Table 2.

Table 3. Nomenclature of the models

Name	Description
Model 1	The base model of two-story
Model 2	Vertically irregular three-story model
Model 3	Regular three-story model

Table 4. Geometrical and material properties of the model

Property	Value
Inter story height	3200 mm
Maximum/Minimum span of the bays	4000 mm/2000 mm
Beam size	230 mm x 330 mm
Slab depth	100 mm
Column size	230 mm x 230 mm
Strength of concrete	20 N mm^{-2}
Poisson's ratio of concrete	0.2
Young's Modulus of Elasticity	22400 N mm^{-2}
Yield Strength of Rebar	500 N mm^{-2}

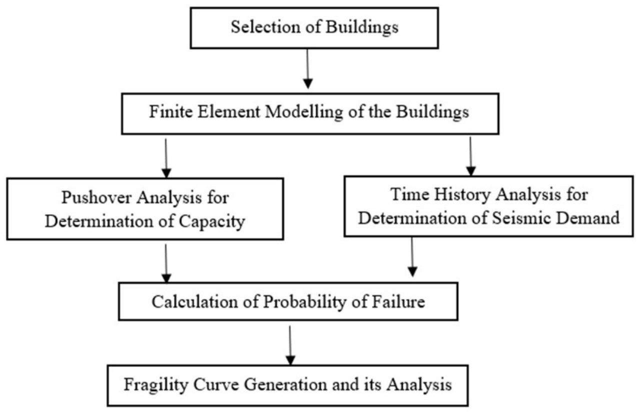

Figure 1 Flowchart of methodology

Linear Time-History analysis was performed to find the demand of the structure. The second-order dynamic equilibrium equation (Equation 1) is given by:

$$[M]\{\ddot{X}\ (t)\} + [C]\{\dot{X}\ (t)\} + [K]\{X(t)\} = \{F(t)\} \quad (1)$$

where *K, C, M,* and *F* are stiffness, damping, diagonal mass, and force matrix. Four different real earthquake accelerograms, i.e., El Centro, Chamauli, Lalitpura, and Gorkha earthquakes were used as seismic loads. For seismic loading, the external loading F(t) was set to zero. The basic equations (Equation 2) for earthquake accelerations can be expressed as follows:

$$[M]\{\ddot{X}\ (t)\} + [C]\{\dot{X}\ (t)\} + [K]\{X(t)\} = -[M]_x\{\ddot{X}\ (t)\}_{xg} - [M]_y\{\ddot{X}\ (t)\}_{yg} - [M]_z\{\ddot{X}\ (t)\}_{zg} \quad (2)$$

From the above Equation 2, the demand of structure was compared in terms of top displacement for all the models, and maximum seismic demand was linearly

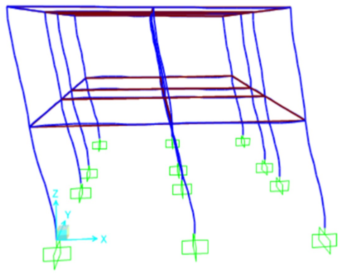

(a) 2-story regular (SAP 2000)

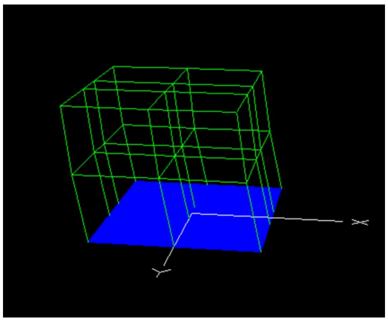

(b) 2-story regular (STERA 3D mode shape)

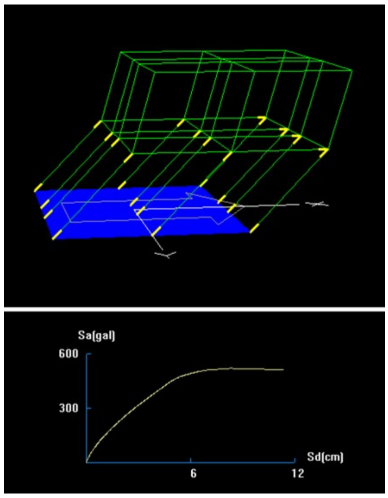

(c) 2-story regular (STERA_3D pushover analysis)

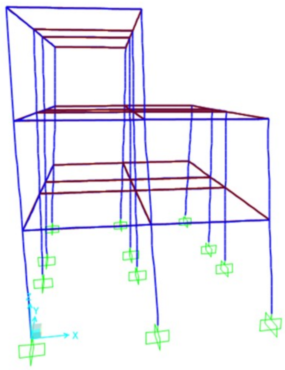

(d) 3-story irregular (SAP 2000)

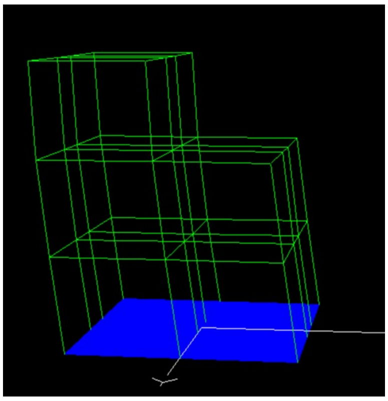

(e) 3-story irregular (STERA 3D mode shape)

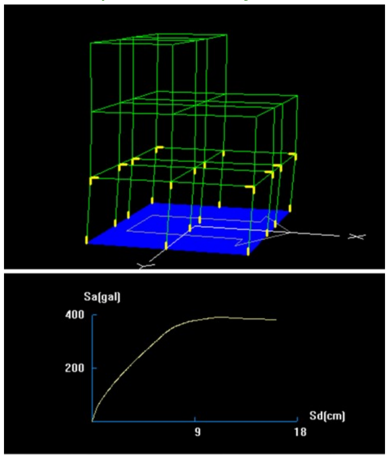

(f) 3-story irregular (STERA_3D pushover analysis)

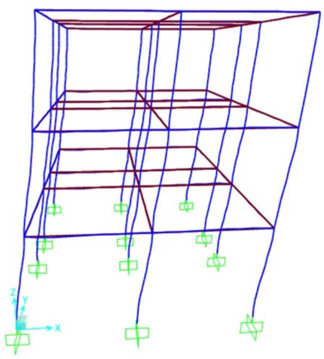

(g) 3-story regular (SAP 2000)

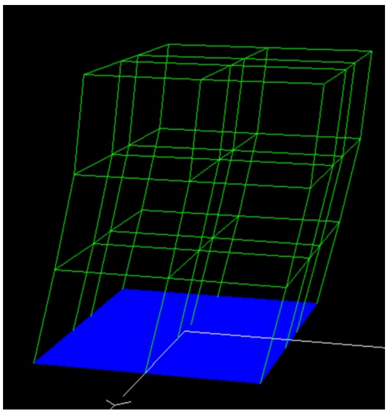

(h) 3-story regular (STERA 3D mode shape)

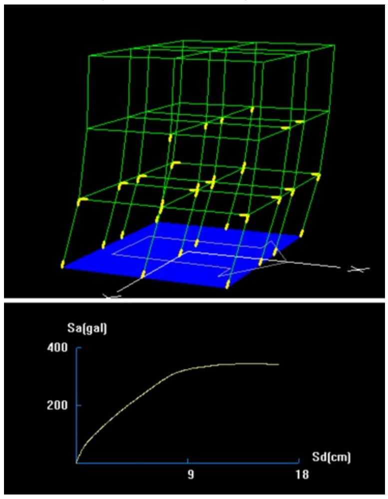

(i) 3-story regular (STERA 3D mode shape)

Figure 2 Models and results of analysis

scaled to different values of peak ground acceleration. Fragility curves were created to establish a relationship between the likelihood of failure (Pf) and the growing demand displacement (*Sd*). These curves were achieved by fitting the equation with the best-suited log-normal distribution function, which was defined by the median

Table 5. Geometrical and material properties of the model

No.	Year	Earthquake Name	Direction	Scaled PGA (in cm s^{-2})
1	1995	JMA Kobe Japan	N-S	414.9
2	1992	Erzican Turkey	N-S	363.8
3	1992	Cape Mendocino Petrolia	0 DEG	470.2
4	1989	Loma Prieta Saratoga-Aloha Ave	0 DEG	520.8
5	1994	Northridge Arleta-Nordhoff Ave Fire Station	90 DEG	446.6
6	1935	Helena Montana-01, Carroll College	180 DEG	576.3
7	1938	Northwest Calif-01, Ferndale City Hall	45 DEG	458.7
8	1940	Imperial Valley-02, El Centro Array 9	180 DEG	423.2
9	1952	Kern County, Taft Lincoln School	21 DEG	454.3
10	1966	Parkfield, Cholame - Shandon Array 5	85 DEG	397.2
11	1972	Managua Nicaragua-01, Managua ESSO	90 DEG	476.7

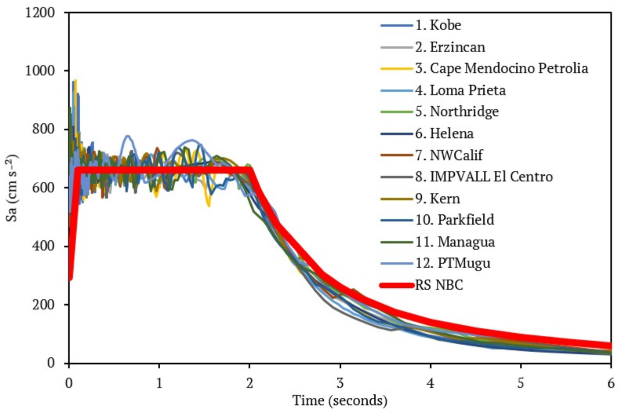

Figure 3 Response spectrum and the matched 11 ground motions

(Sc) and standard deviation (β) parameters (Lumantarna et al., 2006; Hancilar et al., 2014). The intensity measure herein is PGA, as described in Equation 3.

$$P\left[ds/\text{PGA}\right] = \phi\left[\frac{1}{\beta}\ln\left(\frac{\text{PGA}}{Sc}\right)\right] \tag{3}$$

Where ϕ is the cumulative log-normal distribution function and β is the log standard deviation that represents total uncertainty. β equals the sum of the square root of the sum of squares of two different types of variables: uncertainty associated with the threshold for structural damage within the system and the spatial variability of ground motion. The values of which were kept at 0.4 and 0.5 respectively (FEMA, 2003). Fragility curves were derived for four different damage states (Equation 4, 5, 6 and Equation 7), which are as follows (Giovinazzi et al., 2006).

$$\text{Slight},\quad 0.7dy \tag{4}$$

$$\text{Moderate},\quad 1.5dy \tag{5}$$

$$\text{Extensive},\quad 0.5(du+dy) \tag{6}$$

$$\text{Complete},\quad du \tag{7}$$

Where dy and du are the yield ultimate displacement.

The operational performance (I.O.), immediate occupancy (I.O.), damage control (D.C.), life safety (L.S.), and collapse prevention (C.P.) limits were adopted based on HAZUS MR4 (HAZUS, 2003). This study adopted the L.S. limit as suggested by the seismic design standard NBC 105:2020 for the design of residential buildings.

Similar steps were repeated for vertically irregular non-engineered three-story buildings and regular three-story non-engineered buildings. Fragility curves were constructed for all buildings. These curves were then analyzed meticulously and their respective seismic vulnerability was discussed. The pictorial representation of the entire methodology adopted in this paper is presented in Figure 1.

3 MODELLING AND ANALYSIS

The building was modeled and analyzed using structural analysis software SAP 2000 version 24 and STERA_3D. All three models were named as provided in Table 3. Different geometrical and material properties assigned for the models are presented in Table 4.

The plans of all three models were the same. The 3D views and the analysis results of all models are shown in Figure 2. Modal analysis was carried out in both SAP 2000 and STERA_3D. The results from both tools were almost the same as shown in Figure 2.

Staircases were not modeled for convenience and rigid diaphragms were allocated for the slab. Earthquake load was applied according to I.S. 1893:2016 (Indian Standard, 2016) with a seismic zone factor of Zone V. The live load was set at 0.002 N mm^{-2} and the roof live load was set at 0.0015 N mm^{-2}. As per clause 16.2.2 of ASCE 7-16 (ASCE, 2016), at least three ground motions should be selected for time history analysis. In this study, 11 different earthquakes with varying

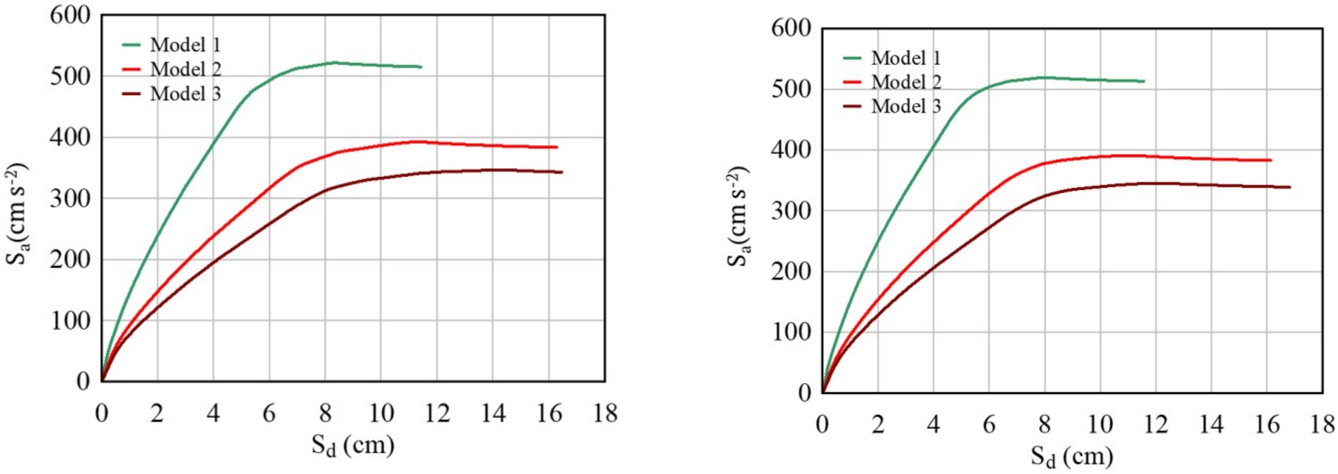

(a) X direction

(b) Y direction

Figure 4 Pushover curves for X and Y-directions

peak ground acceleration were applied in all three models to calculate the maximum seismic demand. The peak ground accelerations of selected real earthquakes are presented in Table 5 (Basukala and Maskey, 2017; USGS, 2021).

Additionally, input ground motions were selected based on the research by (Bhusal et al., 2022) and ATC 40 (ATC, 1996) guidelines. These motions covered a range of Peak Ground Acceleration (PGA) values from 0.12 to 0.35 g, with the targeted PGA for the area being 0.35 g. The selected ground motions were scaled accordingly to meet the target. After scaling, the average response spectrum closely matched the desired requirements. This scaled ground motion can be used to create Incremental Dynamic Analysis (IDA) curves and fragility curves for the study's development. The authors would like to request the readers to study the research of (Bhusal et al., 2022) for further details. The response spectrum of NBC 105:2020 (NBC, 2020) and the matching is shown in Figure 3.

4 RESULTS AND DISCUSSIONS

The performance of the studied building was investigated based on the pushover curves as shown in Figure 4. From Figure 4, it can be observed that the stiffness of the 2 story building is higher compared to the 3 story building.

In this study, the probability of failure (Pf) was calculated as per Equation 3. Fragility curves were then constructed after linearly scaling the seismic demand and the probability of failure of all three models was meticulously compared. The fragility curves of all the models are presented in Figures 5, 6, and 7.

Fragility functions were developed with four damage states, which are represented in Figures 5, 6, and 7.

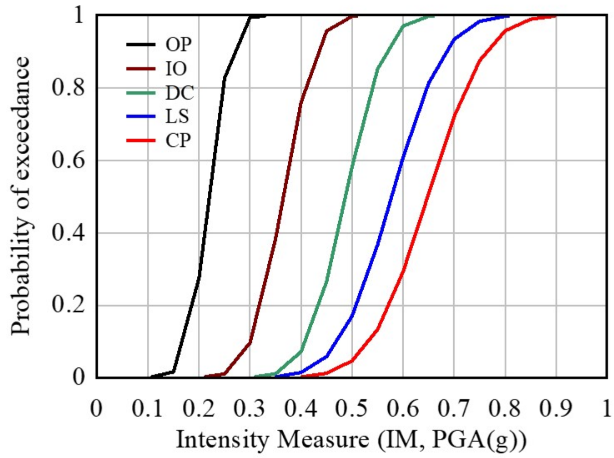

Figure 5 Fragility curve of model 1

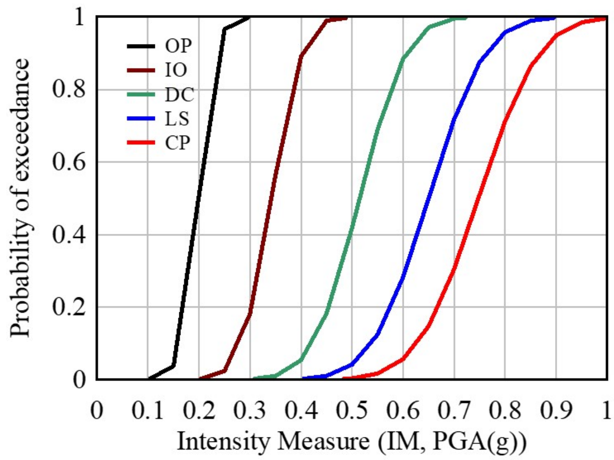

Figure 6 Fragility curve of model 2

These fragility curves represent the probability of failure of the buildings for varying peak ground acceleration of different earthquakes at 0.1g intervals. These curves provide valuable insight for designers to understand the current seismic vulnerability state of the

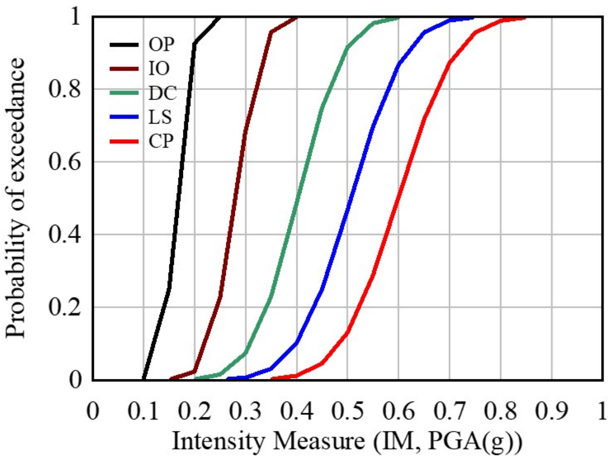

Figure 7 Fragility curve of model 3

Table 6. Probability of failure at 0.4 g for all Models

Models	LS	CP
Model 1	14%	0.5%
Model 2	1.9%	1.5%
Model 3	10%	1.2%

buildings. The seismic hazard map of Nepal proposed by Parajuli et al. (2021) designates that the PGA value of Pokhara for a 10% probability of exceedance in 50 years was anticipated to be 0.4 *g*. Therefore, the probability of failure of the building at various damage states was assessed at 0.4 *g* PGA. The maximum peak ground acceleration (PGA) for a 10% exceedance probability in 50 years in Nepal is 0.4*g* (MoUD, 2020). Hence, for all three different structures, the probability of failure is compared for PGA of 0.4*g* in Table 6.

From Figures 5, 6, and 7, all three models exhibit a very high probability of slight failure with probabilities exceeding 90%. Moderate failure is also highly expected in all three models with probabilities exceeding 50%. However, the change in probability of moderate failure is significant ranging from 66.3% to 79.5% for the non-engineered regular two-story building to the non-engineered vertically irregular three-story building. A prominent variation is observed in the case of extensive failure. It can be observed that the probability of extensive failure doubles in the case of the non-engineered vertically regular three-story building and increases by nearly five times in the case of the non-engineered vertically irregular three-story building, as compared to the vertically regular two-story building. The variation of damage is significant in the case of complete failure as well. The probability of complete failure increases when adding a story irregularly to a non-engineered regular two-story building.

5 CONCLUSION

The comparison of the probability of failure of three different building models through the construction of fragility curves. These curves will be useful for pre-disaster preparedness and loss estimation for possible future earthquake events. They will also aid in decision-making regarding the necessary repair and retrofitting works in the future. The major conclusions of this workstudy are listed below:

a. Fragility curves differ depending on the variations in building geometry and modal frequency.
b. Moderate failure is expected in all three buildings, but the probability of moderate failure is higher in a vertically irregular three-story building compared to a regular three-story building.
c. The probability of extensive failure increases when adding another regular story to the regular two-story non-engineered building. Such probability increases by nearly five fold for a vertically irregular non-engineered three-story building.
d. The probability of complete failure increases from 1.8% to 5.7% when an additional story is constructed vertically irregular rather than vertically regular in the non-engineered two-story building.
e. Variations in top displacement occurred in all three buildings for different earthquakes, possibly associated with variations in the duration and frequency of the earthquake.
f. This study attempts to quantify the probability of failure of the residential building with vertical irregularity only. For further study, it is recommended to compute the probability of failure while considering other irregularities in combination as well for both residential and commercial buildings which might represent a more accurate vulnerability state.

DISCLAIMER

The authors declare no conflict of interest.

ACKNOWLEDGMENTS

The first author would like to express gratitude towards his spouse Kushum Kshetri and brother Mr. Santosh Paudel for their continuous encouragement and technical support during the finalization of the paper.

REFERENCES

ACI (2014), *ACI 318 R-14: Building Code Requirements for Structural Concrete and Commentary on Building Code Requirements for Structural Concrete*, American Concrete Institute, Texas, United States.

ASCE (2016), *ASCE 7-16: Minimum Design Loads and Associated Criteria for Buildings and Other Structures*, American Society of Civil Engineers, Virginia, United States.

ASCE (2017), *ASCE 41-17: Seismic Evaluation and Retrofit of Existing Building*, American Society of Civil Engineers, Virginia, United States.

ATC (1996), *ATC 40: Seismic Evaluation and Retrofit of Concrete Buildings*, Applied Technology Council, Redwood City, California, United States.

Basukala, S. S. and Maskey, P. N. (2017), 'Seismic vulnerability of traditional masonry building: A case study of Byasi, Bhaktapur', *Journal of Science and Engineering* **4**, 24–30.
URL: *https://doi.org/10.3126/jsce.v4i0.22377*

Bhusal, B., Aaqib, M., Paudel, S. and Parajuli, H. R. (2022), 'Site specific seismic hazard analysis of monumental site Dharahara, Kathmandu, Nepal', *Geomatics, Natural Hazards and Risk* **13**(1), 2674–2696.
URL: *https://doi.org/10.1080/19475705.2022.2130109*

Bhusal, B. and Paudel, S. (2021), 'Comparative study of existing and revised codal provisions adopted in nepal for analysis and design of reinforced concrete structure', *International Journal of Advanced Engineering and Management* **6**(1), 25–42.

Bhusal, B., Paudel, S. and Katuwal, T. B. (2020), 'Investigation of confinement effects for determining moment curvature and interaction diagram of reinforced concrete column', *Technical Journal* **2**(1), 81–88.
URL: *https://doi.org/10.3126/tj.v2i1.32844*

Bhusal, B., Paudel, S., Tanapornraweekit, G., Maskey, P. N. and Tangtermsirikul, S. (2023), 'Seismic performance evaluation and strengthening of R.C. beam-column joints adopted in Nepal', *Engineering Structures* **57**, 105205.
URL: *https://doi.org/10.1016/j.istruc.2023.105205*

FEMA (2003), *HAZUS-MH MR3: Multi-hazard Loss Estimation Methodology*, Federal Emergency Management Agency, Washington, United States.

Gautam, D. and Rodrigues, H. (2018), 'Seismic vulnerability of vernacular Newari buildings in Nepal: observations and analysis of damage due to 1934, 1988, 2011, and 2015 earthquakes', *Natural Hazard and Earth System Sciences* .
URL: *https://doi.org/10.5194/nhess-2017-435*

Giovinazzi, S., Lagomarsino, S. and Resemini, S. (2006), 'Displacement capacity of ancient structures through non-linear kinematic and dynamic analyses', *Structural Analysis of Historical Constructions* .
URL: *http://hdl.handle.net/10092/4127*

Hancilar, U., Cakti, E., Erdik, M., Franco, G. E. and Deodatis, G. (2014), 'Earthquake vulnerability of school buildings: Probabilistic structural fragility analyses', *Soil Dynamics and Earthquake Engineering* **67**, 169–178.
URL: *https://doi.org/10.1016/j.soildyn.2014.09.005*

HAZUS (2003), *Technical Manual: Multihazard Loss Estimation Methodology*, Department of Homeland Security, Washington, DC, USA.

Indian Standard (1993), *IS 13920: Ductile Design and Detailing of Reinforced Concrete Structures Subjected to Seismic Force*, Bureau of Indian Standards, New Delhi, India.

Indian Standard (2016), *IS 1893-2016: Criteria for Earthquake Resistant Design of Structures*, Bureau of Indian Standards, New Delhi, India.

Kiyono, J., Furukawa, A., Parajuli, H. R., Maskey, P. N. and Parajuli, R. R. (2017), Vulnerability assessment of historical structures in Kathmandu, Nepal, *in* '16th World Conference on Earthquake', Santiago, Chile.

Lumantarna, E., Griffith, M. C., Vaculik, J. and Lam, N. (2006), 'Seismic fragility curves for unreinforced masonry walls', *Earthquake Engineering in Australia* .
URL: *https://hdl.handle.net/2440/35875*

Motra, G. B. and Paudel, S. (2021), 'Performance evaluation of strengthening options for institutional brick masonry buildings: A case study of Pulchowk Campus', *Progress in Disaster Science* **10**, 100173.
URL: *https://doi.org/10.1016/j.pdisas.2021.100173*

MoUD (2020), *Seismic Design of Buildings in Nepal*, Ministry of Urban Development, Kathmandu, Nepal.

NBC (1994*a*), *NBC 105-1994: Seismic Design of Building in Nepal*, Nepal National Building Code, Kathmandu, Nepal.

NBC (1994*b*), *NBC 205-1994: Mandatory Rules of Thumb Reinforced Concrete Buildings Without Masonry Infill*, Nepal National Building Code, Kathmandu, Nepal.

NBC (2012), *NBC 205-2012: Mandatory Rules of Thumb Reinforced Concrete Buildings Without Masonry Infill*, Nepal National Building Code, Kathmandu, Nepal.

NBC (2020), *NBC 105-2020: Seismic Design of Building in Nepal*, Nepal National Building Code, Kathmandu, Nepal.

NPC (2015), *Nepal Earthquake 2015: Post Disaster Needs Assessment*, Kathmandu, Nepal.

Parajuli, H. R., Bhusal, B. and Paudel, S. (2021), 'Seismic zonation of Nepal using probabilistic seismic hazard analysis', *Arabian Journal of Geosciences* **14**, 2090.
URL: *https://doi.org/10.1007/s12517-021-08475-4*

Paudel, S. (2023), 'Investigation of modelling approaches to study the structural performance of 3D printed plain wall under uniform axial compression', *Advances in Structural Engineering* **26**(10), 1911–1928.
URL: *https://doi.org/10.1177/13694332231166566*

Paudel, S. and Bhusal, B. (2021), 'Investigation of modelling approaches for non-linear analysis of reinforced concrete frames', *Journal of Engineering Science & Technology Review* **14**(2), 61–72.
URL: *https doi:10.25103/jestr.142.09*

Paudel, S., Tanapornraweekit, G. and Tangtermsirikul, S. (2022*a*), 'Numerical investigation of concrete filled hollow precast composite columns subjected to lateral cyclic loading', *Engineering Structures* **252**, 113586.
URL: *https://doi.org/10.1016/j.engstruct.2021.113586*

Paudel, S., Tanapornraweekit, G. and Tangtermsirikul, S. (2022*b*), 'Numerical study on seismic performance improvement of composite wide beam-column interior joints', *Journal of Building Engineering* **46**, 103637.
URL: *https://doi.org/10.1016/j.jobe.2021.103637*

Saito, T. (2020), *STERA 3D: Structural Earthquake Response Analysis D*, Vol. 3, Toyohasi, Japan.

Shrestha, S., Shrestha, B., Shakya, M. and Maskey, P. N. (2017), 'Damage assessment of cultural heritages in Nepal after 2015 Gorkha earthquake: A case study of Jagannath Temple', *Earthquake Spectra* **33**(1), 363–376.
URL: *https://doi.org/10.1193/121616eqs241m*

Tanapornraweekit, G., Jiramarootapong, P., Paudel, S., Tangtermsirikul, S. and Snguanyat, C. (2022), 'Experimental and numerical investigation of 3D-printed mortar walls under uniform axial compression', *Construction and Building Materials* **360**, 129552.
URL: *https://doi.org/10.1016/j.conbuildmat.2022.129552*

TEC (2007), *TEC 2007: Turkish Earthquake Design Code TEC 2007*, Turkish Republic the Ministry of Public Works and Settlement, Ankara, Turkey.

USGS (2021), 'https://www.usgs.gov/natural-hazards/earthquake-hazards/earthquakes'.

World Bank (2017), *Climbing Higher: Toward A Middle Income Nepal*, World Bank Group.

[This page is intentionally left blank]